LBL-36206
UC-413

Lawrence Berkeley Laboratory
UNIVERSITY OF CALIFORNIA

Presented at the Fourth KINR International Conference on Nuclear Physics, Kiev, Russia, August 29–September 7, 1994, and to be published in the Proceedings

Excitation of a Quantal and a Classical Gas in a Time-Dependent Potential

J. Błocki, F. Brut, J. Skalski, and W.J. Świątecki

September 1994

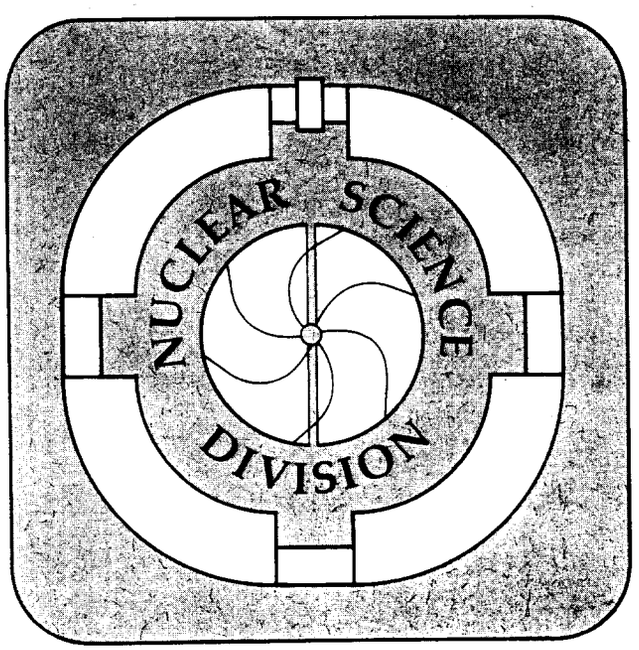

Prepared for the U.S. Department of Energy under Contract Number DE-AC03-76SF00098

LBL-36206
UC-413

Excitation of a Quantal and a Classical Gas in a Time-Dependent Potential*

J. Błocki,[1] F. Brut,[2] J. Skalski,[3] and W.J. Świątecki[4]

[1]Institute for Nuclear Studies, 05-400 Świerk, Poland
[2]Institut des Sciences Nucleaires, 38026 Grenoble-Cedex, France
[3]Institute for Nuclear Studies, Warsaw, Poland
[4]Nuclear Science Division, Lawrence Berkeley Laboratory,
University of California, Berkeley, CA 94720

September 28, 1994

Abstract

We report on computer simulations of oscillating Woods-Saxon or cavity potentials filled with either a classical or a quantal gas of independent particles. We have now available of the order of 600 excitation histories of such gases undergoing usually one period of oscillation (but sometimes several), classified according to frequency and multipolarity of the oscillation and of the degree of diffuseness of the potential. We are still in the process of displaying and interpreting some of the results, but certain important features are already apparent. A notable finding is that, contrary to concerns sometimes voiced in the literature, the classical wall formula [1] does not fail catastrophically when confronted with quantal calculations. This is true even for relatively small systems—in our case 112 neutrons in doubly degenerate eigenstates. On the contrary, the wall formula, in addition to reproducing accurately the classical computer simulations, gives also an approximate account of the quantal results in the regime where it is expected to be valid, namely for not too small oscillation frequencies and not too large surface diffuseness. In those cases it is gratifying to observe that the deviations from the wall formula actually correlate (semi-quantitatively) with the wave-mechanical corrections derived by Koonin et al. [2].

---

*Talk presented by J. Błocki at the Fourth KINR International Conference on Nuclear Physics, Kiev, August 29–September 7, 1994.

1. Introduction

In a previous paper [3] we reported on preliminary results concerning the elastic or dissipative response of a gas in a container to the container's time dependence. Here we present a broad comparison between classical and quantal calculations of the excitation of a gas of independent particles during one period of oscillation, and the results are compared with the predictions of the classical wall formula [1]. In both the classical and quantal calculations two entirely independent numerical codes were developed, one for a diffuse Woods-Saxon potential, the other for a "billiard" or cavity potential with zero diffuseness. Results obtained in a billiard can be directly compared to the wall-formula predictions, whereas those obtained in a Woods-Saxon potential enable us to study in addition the dependence on diffuseness. With the help of those codes we study the behavior of classical and quantal gases in time-dependent integrable shapes like a spheroid, and in non-integrable shapes described by Legendre polynomials P_3, P_4, P_5 and P_6, where the particle trajectories are largely chaotic. (Since at this stage we are more interested in comparing classical and quantal results in well-defined idealized situations rather than in making contact with experiments, we chose the Woods-Saxon potential to be very deep—200 MeV—in order to prevent the escape of particles from the potential well.)

2. Description of the Calculations

2.1. Classical Calculations

In the classical calculations the trajectory of a particle is followed by solving a classical equation of motion. In the case of the billiard, particles between bounces off the container walls move along straight lines. The numerical problem in this case is to find the point in time and space of the collision of a particle with a moving wall. In the case of the diffuse Woods-Saxon potential the equation of motion must be integrated numerically all the way along the trajectory. This integration is performed by a four-point predictor-corrector method. The particles' initial conditions are chosen in a random

Monte Carlo way assuming a uniform distribution in phase space, simulating a density $2/h^3$, where h is a Planck's constant. Thus the filling up of the potential with particles proceeded as follows. At each point in space the particle density is proportional to the third power of the local Fermi momentum, which is proportional to the square root of the depth of the potential with respect to the chemical potential (i.e., the Fermi level). Integrating such a density and equating the result to the number of particles in the quantal case ($N = 112$) we establish the Fermi energy. (This Fermi energy turned out to depend quite significantly on the diffuseness of the potential, being about 45 MeV for a Woods-Saxon diffuseness parameter $a = 0.1$ fm and about 75 MeV for $a = 1.0$ fm. This reflects the fact that the effective radius of the bottom part of the potential well decreases with increasing a.) In order to get good statistics, 20000 trajectories were followed in each case.

2.2. Quantal Calculations

In the quantal calculations we follow the time evolution of 112 uncharged fermions (neutrons) in a billiard or in a Woods-Saxon potential. In both cases the numerical solution is based on an expansion of the wave functions in a suitable basis. In the case of a billiard the basis wavefunctions are eigenfunctions of the spherical billiard, and in the case of a Woods-Saxon potential they are eigenfunctions of a deformed harmonic oscillator. The size of the potential was taken to correspond to a nucleus with $A = 184$ and a radius R_0 equal to $1.16\,A^{1/3}$ fm = 6.5978 fm.

Explicitly, we have

$$V(r,t) = -V_0 \Big/ \left(1 + \exp\left(\frac{r - R(t)}{a}\right)\right) \tag{1}$$

$$R(t) = \frac{R_0}{\lambda(t)}\left(1 + \alpha_n(t) P_n(\cos\theta) + \alpha_1 P_1(\cos\theta)\right) \tag{2}$$

for polynomial deformations, or

$$R(t) = 1 \Big/ \sqrt{(\sin\theta)^2 / b^2 + (\cos\theta)^2 / c^2} \tag{3}$$

for spheroidal deformations, where

$b = R_0/\sqrt{1 + \alpha(t)}$

$c = R_0(1 + \alpha(t))$

Here

$$\alpha_n(t) = \sqrt{\frac{2n+1}{5}}\,(c_0 + c_1 \cos(\omega t)) \quad , \tag{4}$$

where $n = 2, 3, 4, 5, 6$ determines the order of the Legendre polynomial $P_n(\cos\theta)$, and the coefficient c_1 specifies the amplitude of the oscillation around the shape specified by c_0. The factor $\sqrt{\frac{2n+1}{5}}$ ensures that the RMS deviation of the surface from the spherical shape is the same for all n. The factor $\lambda(t)$ ensures volume conservation and $\alpha_1(t)$ ensures fixity of the center of mass in the case of odd polynomials P_n. (For details see Ref. [4].)

In both cases (billiard and a diffuse potential) we first solve the static part of the Schroedinger equation. Due to the axial symmetry the projection m of the angular momentum on the symmetry axis is a good quantum number. In case of reflection symmetry (even Legendre polynomials) the parity π is also preserved. For each m or m^π we calculate single particle energy levels by diagonalizing the hamiltonian. After that we fill up the lowest levels with particles up to $N = 112$, taking into account the degeneracy of the levels, equal to 2 for $m = 0$ and 4 for $m > 0$. The relative excitation energy $(E(t) - E_0)/E_0$ is then followed by solving the time dependent Schroedinger equation using a suitable static deformed oscillator basis (E_0 is the initial energy of the gas).

In the case of the billiard the kinetic energy operator is transformed to new coordinates, $\xi = r/R(\theta)$, θ, ϕ, where r, θ and ϕ are the usual spherical coordinates, and $R(\theta)$ specifies the shape of the axially symmetric cavity. In these new coordinates the cavity is spherical but the kinetic energy operator no longer takes the form of the Laplace operator. In order that a basis fulfill boundary conditions at any instant of time we choose it to be a

set of eigenfunctions of the spherical cavity in the ξ, θ, ϕ variables. Specifically, these eigenfunctions are:

$$\Phi_{m,l,n} = N_{m,l,n} j_l(a_n^l \xi) P_l^m(\cos\theta)\cos(m\phi) \tag{5}$$

where j_l and a_n^l are the spherical Bessel functions and their roots, respectively, P_l^m are the associated Legendre polynomials, $l \geq m$, and $N_{m,l,n}$ are constant normalization factors.

The basis states included in the present calculations were those with $l \leq 19$ and $n \leq 9$, with additional cutoff on the roots of the Bessel functions: $a_n^l \leq 32.5$, which corresponds to the energy of spherical states less than 32.5^2 in units of $2mR_0^2/\hbar^2$. In the same units, the Fermi energy of the system considered is around 100. As an example, the dimension of the basis in the $m = 0$ subspace was 60 for positive parity, and 59 for negative parity states.

In solving the time dependent Schroedinger equation in the case of a diffuse Woods-Saxon potential, there are three parameters which influence the results: the number of oscillator shells N_0, the number of Gauss-Laguerre and Gauss-Hermite integration points used in evaluating the matrix elements of the potential, and the number of time steps. We have checked the convergence of the results as a function of all these parameters. For example, the relative excitation of the gas after one period of the P_4 vibration with an amplitude $\alpha = 0.2$ and $\eta = 0.06$ was 0.0205, 0.0196 and 0.0193 for $N_0 = 18$, 20 and 22. The adiabaticity parameter η is defined as before [4]: $\eta = R_0 c_1 \omega / v_F$, where v_F is the Fermi velocity of particles in the bulk. This parameter defines the ratio of the fastest speed of the wall to the fastest speed of the particles. The number of time steps required to get convergence changes with η. For higher η, fewer time steps are needed. We found that for one period of vibration an adequate number of time steps was 16000 for $\eta = 0.02$ and 800 for $\eta = 0.60$. We do not calculate the matrix elements of the hamiltonian at each time step, but after one hundred time steps for $\eta = 0.02$ and after twenty for $\eta = 0.60$. For the intermediate time steps we calculated the matrix elements by linear interpolation. For the P_4 vibration with $\eta = 0.02$ the relative excitation was 0.062089, 0.059250 and

0.059105 when the number of points N_H at which we calculated the matrix elements was 40, 80 and 160, respectively.

3. Results

In Fig. 1 the quantal results of E_{exc}/E_0 for the spheroid and for the P_4 shape are shown as a function of time for one period of oscillation. The shapes are vibrating around a sphere ($c_0 = 0$) with an amplitude $c_1 = 0.2$ and a frequency ω corresponding to an adiabaticity parameter $\eta = 0.48$. This corresponds to a value of $\hbar\omega$ around 20 MeV. This energy is much higher than the average spacing between single particle levels. We find in this case a characteristic dissipative behavior, especially for the cavity.

The solid curves in Fig. 1 show the predictions of the one-body dissipation formula for a billiard [4], i.e., for a diffuseness $a = 0$. The other curves correspond to the results of quantal calculations for $a = 0$, 0.2, 0.4, 0.6, 0.8, and 1.0 fm. (Increasing diffuseness corresponds to decreasing excitation energy.) As one can see, the results of the calculations are somewhat lower than the one-body predictions even for $a = 0$, and the suppression of the excitation increases with the diffusenesses of the potential.

In Fig. 2 the corresponding classical results are shown. The solid curves correspond again to the predictions of the one-body dissipation formula for $a = 0$ and the other curves are coded as in Fig. 1. The case $a = 0$ fm (closely spaced dots) corresponds to the billiard case, which can be directly compared to the wall formula predictions. As one can see the agreement in this case is close not only for the case of P_4 but also for the spheroid, which for lower values of η is known to show an elastic rather than a dissipative behavior. This seems to be due to the fact that for $\eta = 0.48$ the time for one oscillation allows the particles to make typically only one collision with the wall. This means that there is not enough time for the particles to realize that the potential is integrable.

In Figs. 3 and 4 the quantal and classical values of E_{exc}/E_0 after one period of oscillations are shown for different values of η and different shapes P_3, P_4, P_5 and P_6.

In the quantal case one sees an almost linear dependence of the excitation on diffuseness. In the classical case the dependence on diffuseness is, somewhat unexpectedly, more complicated. We are in the process of analyzing this behavior. The analysis is complicated by the fact noted earlier that increasing the value of a for a very deep potential implies that the value of the effective radius of the lower part of the potential (where the particles reside) is decreased.

Figure 5 summarizes the relative excitations calculated after one period for all multipoles and frequencies (η values) in the case of zero diffuseness. The classical results (squares) agree with the wall formula (solid line) in all cases except for P_2 and the spheroid, which show the expected deviations for small η. The quantal results are systematically below the wall formula prediction. The dashed line is the result of using the following expression derived in [2], which corrects the wall formula for the wave-mechanical suppression of the dissipation due to the finite ratio of the wavelength of the quantized particles to the wavelength of the multipole ripples of the oscillating cavity:

$$\frac{dE}{dt} = \left(\frac{dE}{dt}\right)_{wall}\left[1+\frac{x^2}{8}-\frac{x^2(8+x^2)}{16\left(2+\sqrt{(4-x^2)}\right)}+\frac{x^2}{8}\left(\frac{x^2}{4}-4\right)\ln\left(2+\sqrt{\frac{4-x^2}{x}}\right)\right] \quad , \quad (6)$$

where x = (Fermi wavelength)/(Ripple wavelength).

Acknowledgements

This work was supported in part by the U.S.–Polish Maria Curie-Sklodowska Fund PAA/NSF-91-68, by the Fund KBN-2660/2/91 of the Polish Scientific Committee and by the Director, Office of Energy Research, Division of Nuclear Physics of the Office of High Energy and Nuclear Physics of the U.S. Department of Energy under Contract No. DE-AC03-76SF00098.

References

1. J. Błocki, Y. Boneh, J.R. Nix, J. Randrup, M. Robel, A. Sierk and W.J. Świątecki, Ann. Phys. **113** (1978) 330.
2. S.E. Koonin, R.L. Hatch, and J. Randrup, Nucl. Phys. **A283** (1977) 87.
3. J. Błocki, F. Brut, and W.J. Świątecki, Acta Physica Polonica **B25** (1994) 637.
4. J. Błocki, Y.J. Shi, and W.J. Świątecki, Nucl. Phys. **A554** (1993) 387.

Figure Captions

Fig. 1. The time-dependence of the relative excitation energy of a gas of 112 fermions in a time-dependent potential in the course of one complete period T. The solid curves are the predictions of the classical wall formula, and the other curves are the numerical results for various degrees of diffuseness of the potential, given by $a = 0$ (next highest dissipation), 0.2, 0.4, 0.6, 0.8 and 1.0 fm (lowest dissipation).

Fig. 2. This is like Fig. 1 but for a classical gas. The coding of the curves is the same as in Fig. 1.

Fig. 3. The relative excitation energy of 112 fermions after one period of oscillation, as a function of the diffuseness parameter a, for various speeds of oscillation (as given by η), and for four different polynomial deformations.

Fig. 4. This is like Fig. 3 but for a classical gas.

Fig. 5. The relative excitation energy after one period of oscillation in the case of a (zero diffuseness) billiard potential, for six different shapes. The squares refer to a classical gas and the solid curves are the corresponding predictions of the wall formula. The stars refer to a gas of 112 fermions and the dotted curves refer to the wall formula modified by the wave-mechanical correction from Ref. 2.

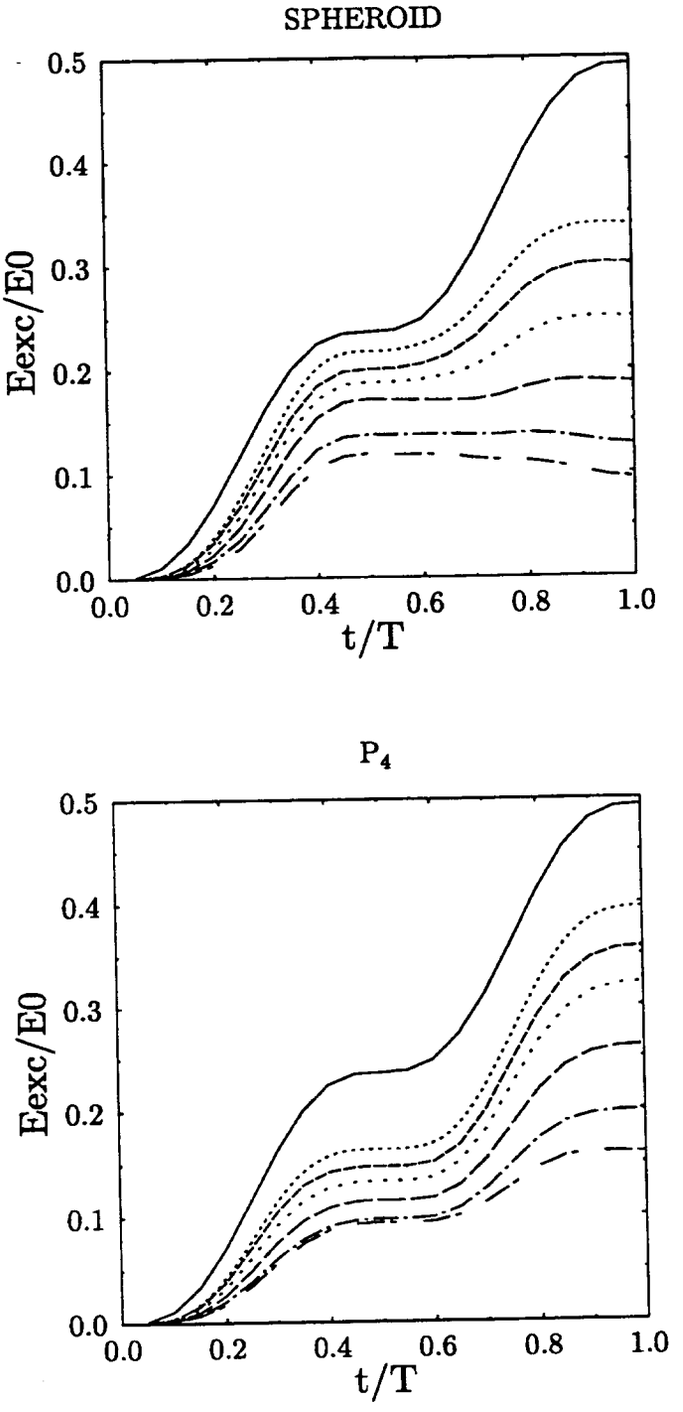

Fig.1

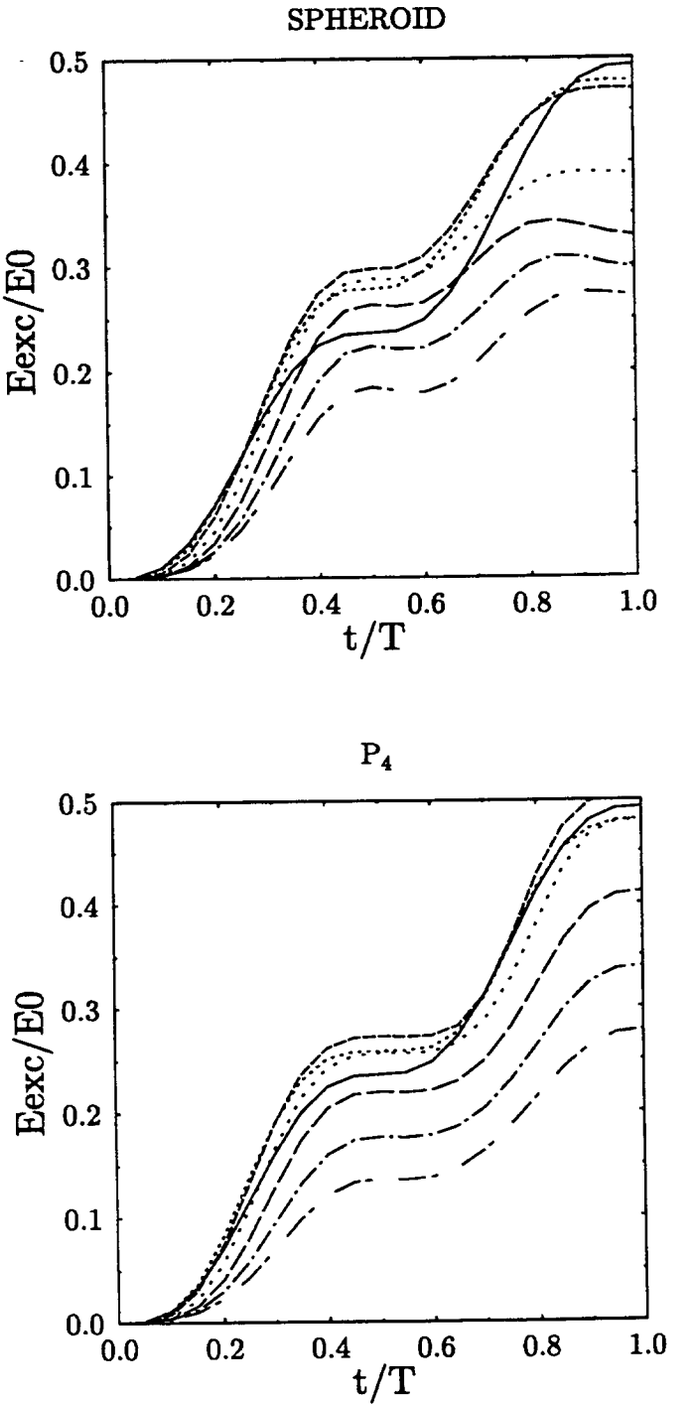

Fig.2

c_1=0.2 V_0=-200 MeV QUANT

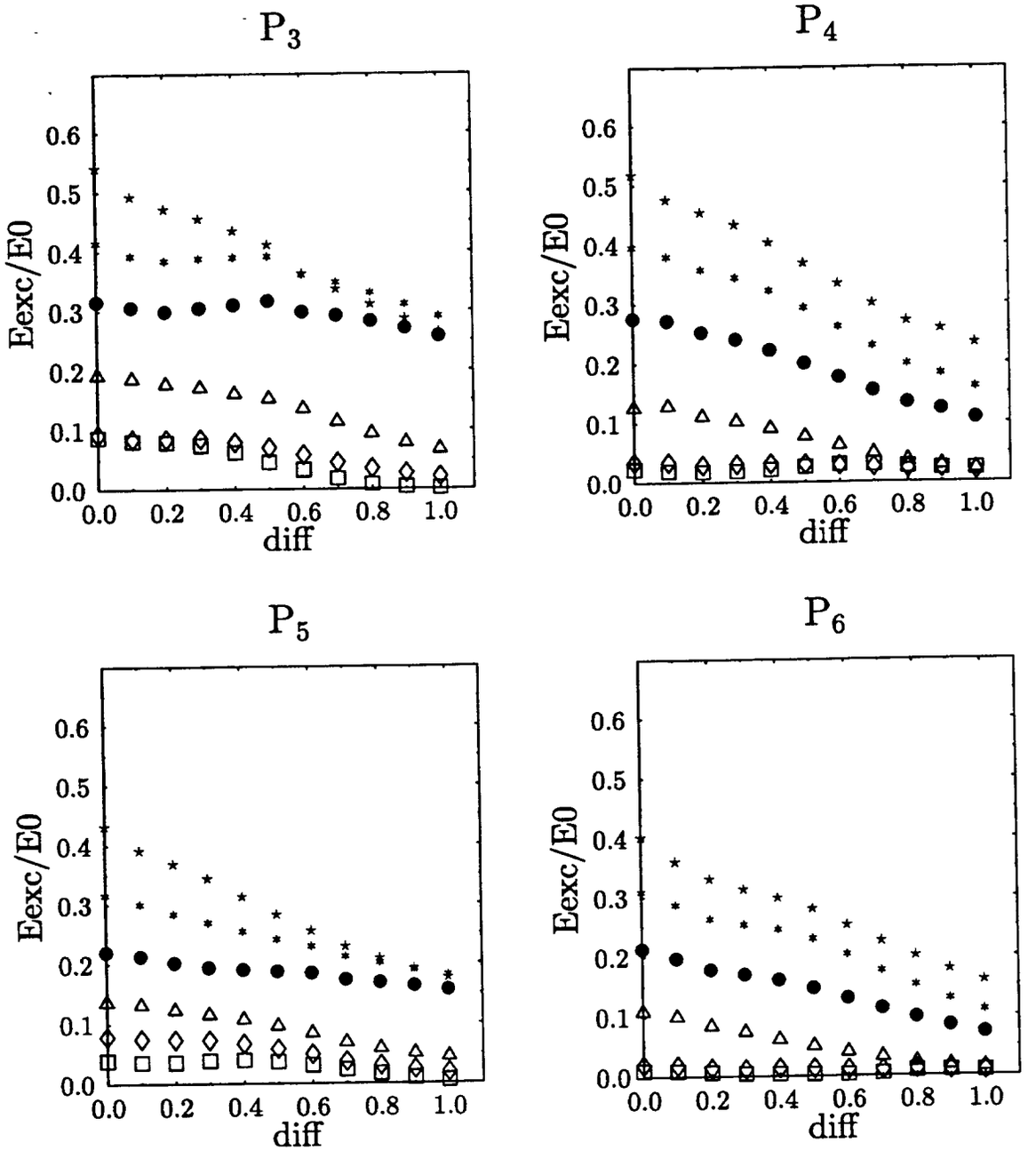

η=0.06 - squares, η=0.12 - diamonds, η=0.24 - triangles
η=0.36 - full circles, η=0.48 - asterix, η=0.60 - stars

Fig.3

c_1=0.2 V_0=-200 MeV CLASS

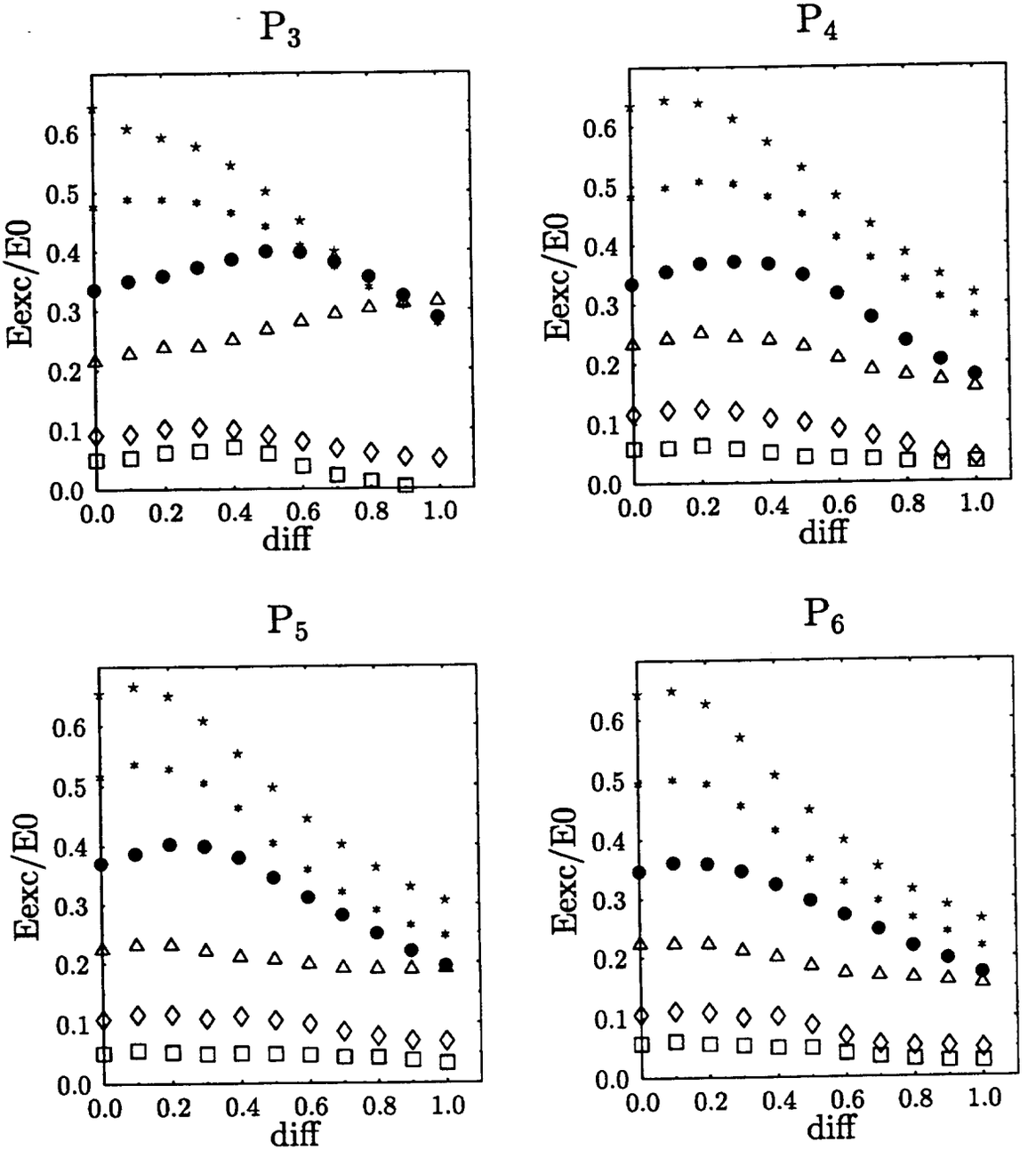

η=0.06 - squares, η=0.12 - diamonds, η=0.24 - triangles
η=0.36 - full circles, η=0.48 - asterix, η=0.60 - stars

Fig.4

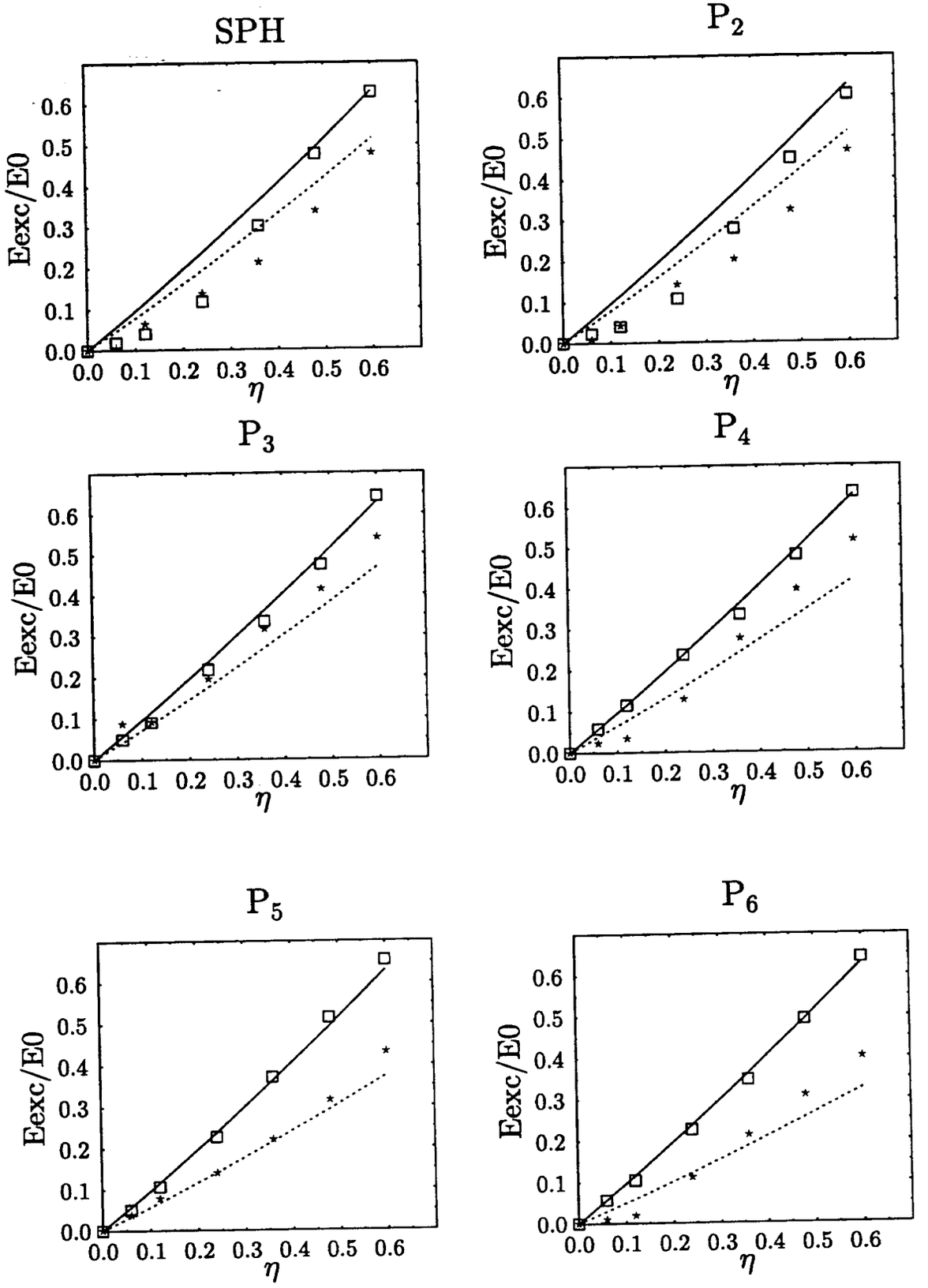

Fig.5